

Study of the Interactions between MeOH and Daidzein at the Molecular Level

Hailiang Zhao, Zhenjun Wu, Yaming Sun, Xue Song, Fan Shi, Yingming Zhang, and Xia Sheng*

Cite This: *ACS Omega* 2021, 6, 21491–21498

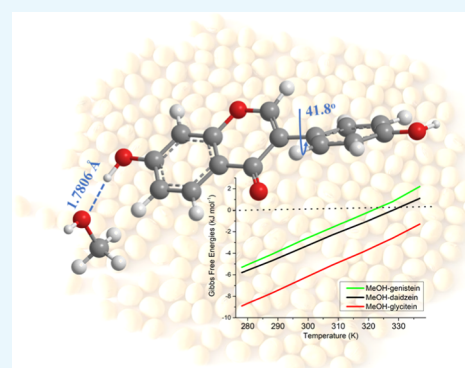
Read Online

ACCESS |

Metrics & More

Article Recommendations

ABSTRACT: In this study, the interactions between daidzein and methanol were studied to investigate isoflavone extraction. The complexes of MeOH–daidzein = 1:1, 2:1, 4:1, and 7:1 were studied using DFT/B3LYP-D3. According to the findings of this study, daidzein can act as a hydrogen bond donor as well as an acceptor. Binding energies demonstrate that more MeOH molecules interacting with daidzein could give more stability to the system. The strengths of the hydrogen bonds reveal that daidzein prefers to act as a hydrogen bond donor than an acceptor. The atoms in molecules (AIM) topological analysis was performed to analyze the nature of the hydrogen bonds. Moreover, daidzein, genistein, and glycitein are the most common soybean isoflavones, and their properties during extraction were also studied. The binding energies show that the soy isoflavone genistein is more reactive with the solvent than daidzein, followed by glycitein. The extraction conditions of the three common soy isoflavones in MeOH solution were obtained at 321, 328, and 348 K for genistein, daidzein, and glycitein, respectively. The generalized Kohn–Sham energy decomposition analysis (GKS-EDA) results indicate that the solute–solvent molecular interactions are typical hydrogen bonds with predominantly electrostatic and exchange energies in nature.



1. INTRODUCTION

Isoflavones are oxygen heterocyclic compounds, which have a 3-phenylchroman skeleton that is hydroxylated at the 4 and 7 positions.¹ They are classified under natural products that are imbued with numerous biological benefits including their antioxidant abilities and anticancer properties, which make them important for both commercial use and physical consumption.^{1,2} Daidzein (C₁₅H₁₀O₄) structurally belongs to isoflavones, and it is a naturally occurring compound found exclusively in soybeans and other legumes.^{3,4} It exhibits similar structural and functional qualities to those of the human mammalian endogenous hormone estrogen and therefore is also known as one of the most common phytoestrogens. Consequently, daidzein plays a paramount role in hormone replacement therapy (HRT) for women who are undergoing menopause.⁵

To access the benefits of isoflavones, choosing an appropriate solvent is of tremendous importance for isoflavone extraction. It has always been known that the hydrogen bonds between a solute and polar organic solvent play a crucial role in selective extraction.⁶ In particular, the hydroxyl and carbonyl groups in isoflavones have been demonstrated to strongly interact with solvents via hydrogen bonds.^{7,8} Thus, methanol (MeOH), ethanol (EtOH), acetonitrile (MeCN), etc. have been commonly used to extract isoflavones.^{9–11} In a previous experimental study, Zuo et al. recovered up to 87.3% of isoflavones with aqueous MeOH-modified supercritical carbon

dioxide.¹² Luthria et al. also studied the interaction between daidzein and a solvent mixture (v/v, 90:10, MeOH–H₂O), and they could recover 100% daidzein from soybeans.¹³ This is because the hydrogen bond between the solute and polar organic solvent plays a crucial role in selective extraction.⁶ However, the interactions between the solute and the solvent are still not fully understood from a molecular level. Since daidzein is an important isoflavone from soybeans, understanding the interactions between the solute and solvent would be crucial to reveal the isoflavone extraction.

In this study, the interactions between MeOH and daidzein were investigated using density functional theory (DFT). Moreover, daidzein, glycitein, and genistein are the three major isoflavones in soybeans, and they can account for up to about 3 mg g⁻¹ (dry weight) in soybeans.¹⁴ Their structure and functions are very similar to each other. The extraction competition among daidzein, glycitein, and genistein was further analyzed.

Received: May 5, 2021

Accepted: August 3, 2021

Published: August 11, 2021



2. RESULTS AND DISCUSSION

As shown in Figure 1, the isolated daidzein molecule is very similar to glycitein and genistein. The structural differences are

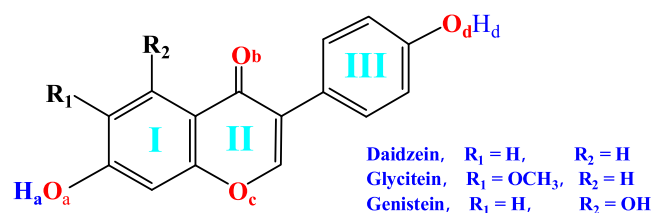


Figure 1. Molecular structures of the three soybean isoflavone aglycone homologues: daidzein, glycitein, and genistein.

the groups of R_1 and R_2 . For daidzein, both R_1 and R_2 are hydrogen atoms. The structure of daidzein is such that the III ring slightly rotates out of the plane formed by the rings I and II, causing it to exhibit a nonplanar structure. Thus, this results in a torsion angle between the II and III rings, and it was approximately calculated to be 41.0° , which is in good agreement with those of glycitein ($40.9\text{--}41.9^\circ$) and genistein ($42.0\text{--}43.3^\circ$).^{7,8} However, the calculated torsion angle is smaller than the value (45.1°) in the single crystal structure.¹⁵ This is due to the intermolecular hydrogen-bonding interactions between the phenolic hydroxyl group and carbonyl group in the crystal lattice.

Daidzein has four different oxygen atoms, namely, O_a , O_b , O_c , and O_d (Figure 1). These four oxygen atoms in daidzein are engaged with three types of oxygen. The O_a atom together with the O_d atom belongs to a hydroxyl group. O_b is derived from a carbonyl group, and O_c , on the other hand, belongs to an ether group. Moreover, the rotation of the O_aH_a and O_dH_d groups results in four conformers (Figure 2). However, the

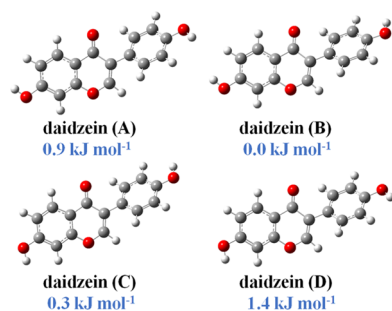


Figure 2. Optimized four daidzein stable conformers at the B3LYP-D3/cc-pVTZ level. Relative electronic energies are listed with respect to the daidzein (B) conformer.

four conformers are very close in electronic energy, with the daidzein (B) conformer as the most stable one. This means that the rotation of the OH groups only slightly affects the stabilities of daidzein. In contrast, the daidzein (C) conformer was found to be the most stable one in the crystal lattice.¹⁵ This is because the intermolecular interactions of solute–solute and solute–solvent normally play a significant role in determining the phase transformation of substances and mixtures.^{16–18} However, the energy difference between the daidzein (B) and the daidzein (C) conformers is very small ($\sim 0.3 \text{ kJ mol}^{-1}$). To be consistent with the experimental data, the daidzein (C) conformer was used to investigate the solute–solute and solute–solvent interactions.

2.1. Solute–Solvent Intermolecular Interactions.

During extraction, the solvent molecules (such as MeOH) can interact with the solute. As seen from Figure 1, there are two possible ways for the interaction between MeOH and daidzein, namely, as either a hydrogen bond acceptor or a hydrogen bond donor. MeOH–daidzein has two types of hydrogen-bonding interactions: $\text{O} \cdots \text{H} \cdots \text{O} \cdots \text{H}$ and $\text{O} \cdots \text{H} \cdots \text{O} = \text{C}$. The stable structures of the MeOH–daidzein complexes at the B3LYP-D3/cc-pVTZ level are displayed in Figure 3. Table

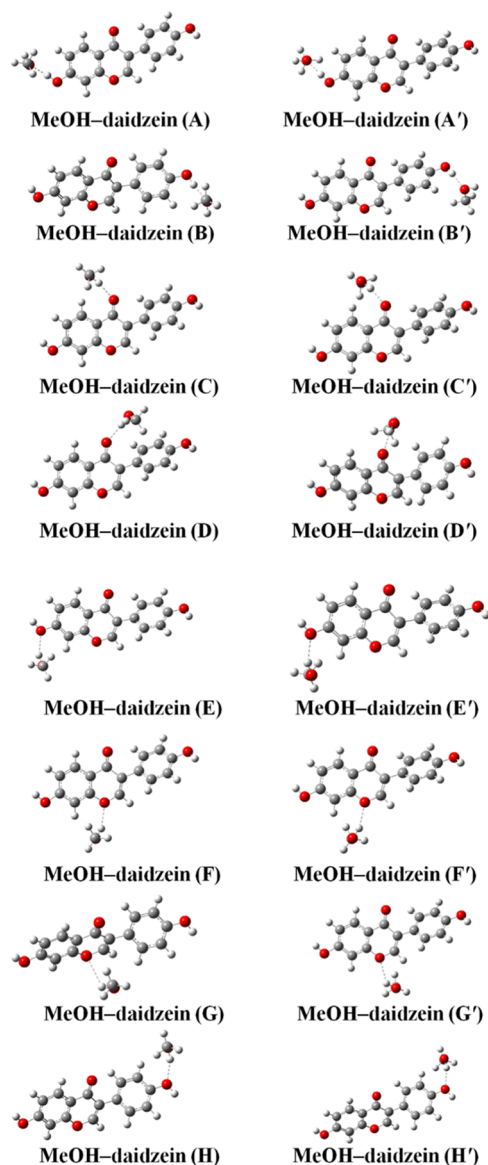


Figure 3. Stable structures of the MeOH–daidzein complexes at the B3LYP-D3/cc-pVTZ level. Hydrogen bonds between MeOH and daidzein are represented by dashed lines.

1 is a presentation of the calculated binding energy (BE), enthalpy of formation ($\Delta H_{298\text{K}}^\circ$), and Gibbs free energy of formation ($\Delta G_{298\text{K}}^\circ$) for the MeOH–daidzein complexes at the B3LYP-D3/cc-pVTZ level. The binding energies are in the range of -40.3 to $-19.2 \text{ kJ mol}^{-1}$. The binding energies are significantly negative, which indicates the stability of the daidzein-containing complexes. Previous studies on the calculations of solvation free energy also showed that daidzein

Table 1. Calculated Binding Energy (BE), Zero-Point Vibrational Energy (ZPVE), Enthalpy of Formation (ΔH_{298K}^θ), and Gibbs Free Energy of Formation (ΔG_{298K}^θ) at 298.15 K and 1 atm for the Daidzein-Containing Complexes at the B3LYP-D3/cc-pVTZ Level^a

conformer	BE ^b	ZPVE	ΔG_{298K}^θ	ΔH_{298K}^θ
MeOH–daidzein (A)	−39.6	5.6	−3.5	−38.4
MeOH–daidzein (A')	−40.3	6.2	−2.9	−39.5
MeOH–daidzein (B)	−35.2	5.6	1.2	−34.1
MeOH–daidzein (B')	−35.8	6.2	2.0	−35.1
MeOH–daidzein (C)	−37.6	5.6	0.1	−36.8
MeOH–daidzein (C')	−37.4	5.6	0.5	−36.6
MeOH–daidzein (D)	−35.6	5.2	5.2	−35.0
MeOH–daidzein (D')	−34.5	5.1	4.7	−33.7
MeOH–daidzein (E)	−23.0	4.6	13.5	−21.6
MeOH–daidzein (E')	−23.0	4.6	13.7	−21.6
MeOH–daidzein (F)	−19.8	4.3	16.4	−18.2
MeOH–daidzein (F')	−19.9	4.4	16.3	−18.3
MeOH–daidzein (G)	−22.9	3.7	13.9	−21.0
MeOH–daidzein (G')	−19.2	3.8	15.0	−17.3
MeOH–daidzein (H)	−24.0	4.8	12.5	−22.7
MeOH–daidzein (H')	−23.7	4.7	12.7	−22.4

^aEnergies are in kJ mol^{-1} . ^bBEs are corrected with ZPVE.

had a very strong solute–solvent interaction ($\sim 64.0 \text{ kJ mol}^{-1}$) with the MeOH solvent.¹⁵

In the MeOH-containing complexes, BEs were obtained at -21.2 to $-19.7 \text{ kJ mol}^{-1}$ (B3LYP/aug-cc-pVTZ) when MeOH (as a hydrogen bond donor) interacted with dimethyl ether (DME), dimethylamine (DMA), and trimethylamine (TMA).^{19,20} These are slightly less favored than the MeOH–daidzein complexes (Figure 3C–H,C'–H'; -37.6 to $-19.2 \text{ kJ mol}^{-1}$), where MeOH is the hydrogen bond donor and daidzein is the hydrogen bond acceptor. When MeOH docks on the O_a and O_d sites, the binding energies were obtained at -24.0 to $-23.0 \text{ kJ mol}^{-1}$ (Figure 3E,E',H,H'). In addition, the binding energies were calculated to be -37.6 to $-34.5 \text{ kJ mol}^{-1}$ (Figure 3C,C',D,D') and -22.9 to $-19.2 \text{ kJ mol}^{-1}$ (Figure 3F,F',G,G') for the structures where MeOH approaches O_b and O_c , respectively. Therefore, the strength of the hydrogen bond with daidzein as the hydrogen bond acceptor can be sorted as $O_b > O_a/O_d > O_c$. This is the same conclusion as our previous studies on the hydrogen-bonding interactions between alcohols and methyl esters: the oxygen atom in the carbonyl group is a stronger hydrogen bond acceptor than that in the ester group.²¹

Meanwhile, daidzein can also interact with the solvent as a hydrogen bond donor. The binding energies of the MeOH–daidzein complexes (Figure 3A,A',B,B') were obtained at -40.3 to $-35.2 \text{ kJ mol}^{-1}$. It can be seen that daidzein is a stronger hydrogen bond donor than MeOH. Thus, it can also be concluded that daidzein prefers to act as a hydrogen bond donor than a hydrogen bond acceptor. Meanwhile, daidzein, glycitein, and genistein are three common soybean isoflavones. Our previous studies on the molecular interactions between solvents and solutes showed that the binding energies of the most stable MeOH–genistein and MeOH–glycitein conformers were calculated to be -40.7 and $-37.2 \text{ kJ mol}^{-1}$ (B3LYP-D3/cc-pVTZ, with ZPVE corrections), respectively.^{7,8} In this study, the binding energy of the most stable structure of MeOH–daidzein was calculated to be $-40.3 \text{ kJ mol}^{-1}$. Then, it can be noticed that genistein is more reactive with the solvent

than daidzein, followed by glycitein. This is the same conclusion as stated in a previous experimental study on the distribution coefficients and selectivities of the three soybean isoflavones in 1-butyl-3-methylimidazolium hexafluorophosphate ([Bmim][PF₆]), where the distribution order was obtained to be genistein > daidzein > glycitein.⁶

In solution, multiple solvent molecules can interact with daidzein to form more stable clusters. The systems containing multiple MeOH molecules (MeOH–daidzein = 2:1, 4:1, and 7:1) were further studied. The selected stable structures of the MeOH–daidzein = 2:1 complexes at the B3LYP-D3/cc-pVTZ level are displayed in Figure 4. Since MeOH can act as both a hydrogen bond acceptor and a hydrogen bond donor, the blue-shaded ring is used to represent the hydrogen bond acceptor and the red-shaded square is utilized to represent the hydrogen bond donor to distinguish these two types of interactions. In (MeOH)₂–daidzein (A–F), one MeOH is the hydrogen bond donor and the other MeOH is the hydrogen bond acceptor. In

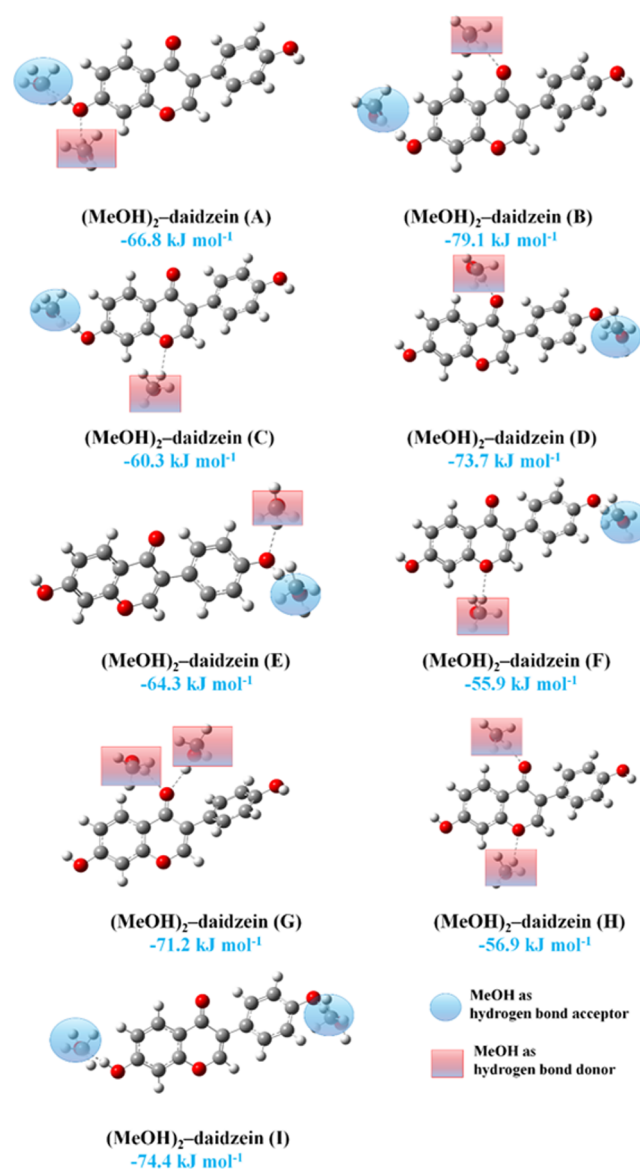


Figure 4. Stable structures of the (MeOH)₂–daidzein complexes at the B3LYP-D3/cc-pVTZ level. Hydrogen bonds between MeOH and daidzein are represented by dashed lines.

(MeOH)₂-daidzein (G-H), the two MeOH molecules are the hydrogen bond donors. On the other hand, the two MeOH molecules are the hydrogen bond acceptors in (MeOH)₂-daidzein (I). The binding energies of the (MeOH)₂-daidzein (A-I) systems were obtained to be -79.1 to -56.9 kJ mol⁻¹. The addition of one extra MeOH to MeOH-daidzein could better stabilize the system. For example, the hydrogen-bonding interactions in (MeOH)₂-daidzein (A) can be considered as the combination of MeOH-daidzein (A) and MeOH-daidzein (E). The binding energy of (MeOH)₂-daidzein (A) was calculated to be -66.8 kJ mol⁻¹, which is much lower than the summation (-62.6 kJ mol⁻¹) of MeOH-genistein (C) (-39.6 kJ mol⁻¹) and MeOH-daidzein (E) (-23.0 kJ mol⁻¹). This implies that adding more MeOH molecules to the daidzein molecule could gain extra stability.

There are four docking sites in the daidzein molecule for the upcoming MeOH. Besides two MeOH molecules, more MeOH molecules can be added into daidzein. The most stable structures of the MeOH-daidzein = 4:1 and 7:1 complexes are displayed in Figure 5. In the (MeOH)₄-

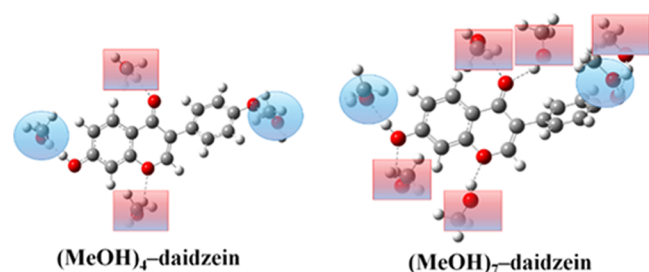


Figure 5. Stable structures of the (MeOH)₄-daidzein and (MeOH)₇-daidzein complexes at the B3LYP-D3/cc-pVTZ level. Hydrogen bonds between MeOH and daidzein are represented by dashed lines.

daidzein system, there are four corresponding MeOH molecules in the four docking sites of daidzein. The binding energy of (MeOH)₄-daidzein was obtained at -134.6 kJ mol⁻¹. The O_c oxygen is a weak hydrogen bond docking site, and it can only interact with one MeOH molecule. On the other hand, the remaining three docking sites in daidzein can accommodate two MeOH molecules in each docking site. Thus, one daidzein molecule can interact with no greater than seven MeOH molecules at the same time. The (MeOH)₇-

daidzein system would be considered as a fully saturated system. The calculated binding energy of (MeOH)₇-daidzein was simulated at -247.7 kJ mol⁻¹.

2.2. Solute-Solute Intermolecular Interactions. The solute-solute interactions were also calculated. The two daidzein molecules tend to bind together by forming two O-H...O=C hydrogen bonds (Figure 6). The two hydrogen-bonded conformers were calculated to be -49.5 to -35.6 kJ mol⁻¹. Meanwhile, the π - π stacking interaction between the chromanone-chromanone layers and benzene-benzene layers was obtained at -64.2 kJ mol⁻¹. Thus, it can be seen that the π - π stacking interactions are much stronger than the hydrogen-bonding interactions. However, the binding energy of the most stable structure of MeOH-daidzein was calculated as -40.3 kJ mol⁻¹, which is less stable than the daidzein-daidzein interactions. Daidzein has several different docking sites, enabling it to form (MeOH)₂-daidzein, (MeOH)₃-daidzein, and so on. Adding more MeOH into the daidzein system can give extra stability.⁸

However, the daidzein-daidzein interactions are hardly observed in solution. They were experimentally observed in the daidzein crystal phase.¹⁵ It could also be interesting to compare the differences of the daidzein-daidzein interactions in solution and crystals. The two types of intermolecular interactions, namely, π - π stacking interactions and hydrogen-bonding interactions, can be directly observed in the crystal (Figure 6).¹⁵ The O-H...O-H and O-H...O=C hydrogen-bonding interactions for the structures taken from the crystal lattice were calculated to be -30.9 and -45.7 kJ mol⁻¹, respectively. The corresponding hydrogen bond distances were measured to be 1.9292 and 1.8826 Å in the crystal for O-H...O-H and O-H...O=C, respectively.¹⁵ The O-H...O-H hydrogen-bonding interactions cannot be found in solution. This is because the O-H...O=C hydrogen-bonding interaction is much stronger than the O-H...O-H hydrogen-bonding interaction. The O-H...O-H hydrogen-bonding interaction in MeOH-MeOH was simulated to be about -22.6 kJ mol⁻¹ (MP2/cc-pV5Z).²² The O-H...O=C bonds were slightly weaker (-35.8 to -29.7 kJ mol⁻¹, B3LYP-D3/aug-cc-pVTZ) and shorter (1.7950-1.8791 Å, B3LYP-D3/aug-cc-pVTZ) for the hydrogen-bonding interactions between 2,2,2-trifluoroethanol (TFE) and the methyl esters (methyl formate, methyl acetate, methyl trifluoroacetate).²¹ In solution, there is much more freedom of movement than in the crystal lattice. The less stable O-H...O-H hydrogen-bonding

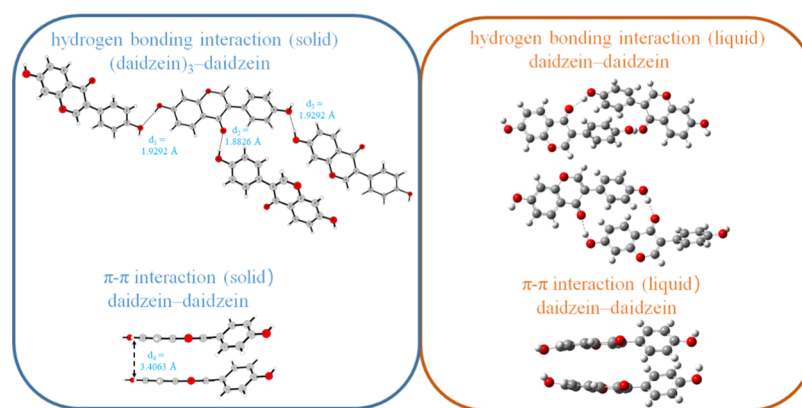


Figure 6. Daidzein-daidzein hydrogen-bonding interactions and π - π interactions in both solid and liquid phases. d_1 , d_2 , and d_3 are the hydrogen bond distances and d_4 is the distance between the two daidzein layers.

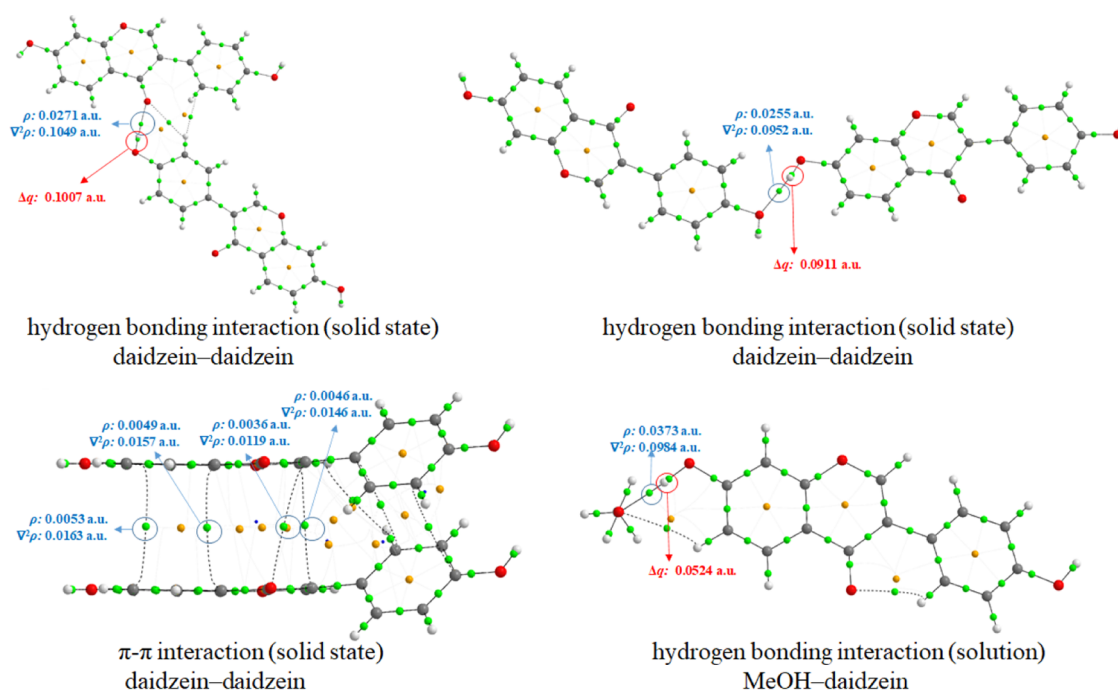


Figure 7. QTAIM molecular graphs of the selected daidzein–daidzein and MeOH–daidzein structures in both solid and solution phases. The solid circles correspond to attractors attributed to atomic positions: white, H; gray, C; and red, O. Small circles are attributed to critical points: green, bond critical point and yellow, ring critical point.

interaction was converted into the more stable O–H···O=C hydrogen-bonding interaction. Besides the hydrogen-bonding interaction, there is also a π – π interaction in the crystal phase. The corresponding π – π interaction for the structures taken from the crystal lattice was obtained at -59.1 kJ mol $^{-1}$. The π – π interactions were found between the chromanone–chromanone layers and benzene–benzene layers with planar distances of about 3.4063 and 3.4968 Å in the crystal, respectively.¹⁵ The π – π interaction distance in the benzene–benzene dimer (sandwich shape) was calculated to be 3.90 Å (CCSD(T)/aug-cc-pVQZ).²³ The corresponding π – π interaction energy was calculated to be about -7.57 to -6.40 kJ mol $^{-1}$, using the CCSD(T) method with the complete basis set (CBS) limit.²⁴ The π – π interaction in this study is much more strong than the π – π interaction in the benzene–benzene dimer, and this is due to the larger π system in daidzein than the one in benzene. The daidzein–daidzein π – π interaction in solution was slightly stronger (-64.2 kJ mol $^{-1}$) than that in the crystal phase (-59.1 kJ mol $^{-1}$).

2.3. Nature of the Hydrogen Bond: QTAIM. Looking at the geometries of the complexes, it is not possible to say that the complexes are formed by electrostatic interactions or by hydrogen-bonding interactions. On the other hand, the Bader's quantum theory of atoms in molecules (QTAIM) method can give criteria for the existence of hydrogen bonds. Based on QTAIM, the chemical bonds in the molecular complexes can be classified by the electron density at bond critical points.²⁵ The charge density $\rho(r)$ and the Laplacian of charge density $\nabla^2\rho(r)$ at bond critical points (BCPs) are normally used to distinguish between noncovalent closed-shell interactions (van der Waals' interactions, hydrogen bonds, ionic bonds, etc.) and covalent ones.²⁵ Then, the chemical bonds can be classified as noncovalent closed-shell interactions ($\nabla^2\rho(r) > 0$) or covalent ones ($\nabla^2\rho(r) < 0$). The QTAIM molecular graphs of the selected daidzein-containing structures in both solid and liquid

phases are shown in Figure 7. Moreover, a hydrogen bond exists if the electron density $\rho(\text{BCP})$ values at bond critical points (BCPs) are 0.002–0.040 au and the Laplacian of charge density $\nabla^2\rho(\text{BCP})$ values at BCPs are 0.014–0.139 au.^{25,26} The $\rho(\text{BCP})$ values in the hydrogen-bonding interactions are in the range of 0.0255–0.0373 au, and the $\nabla^2\rho(\text{BCP})$ values are about 0.0952–0.1049 au (Figure 7). Thus, these interactions are typical hydrogen bonds. In addition, there are also some C–H···O hydrogen bonds as shown in Figure 7. These interactions are weak noncovalent ones. They are known as cooperative hydrogen-bonding interactions, which play important roles in molecular structures.^{27,28} Furthermore, a charge normally transfers from the hydrogen bond acceptor to the hydrogen bond donor.²⁹ Thus, the QTAIM atomic charges on the H atoms ($\Delta q(\text{H})$) upon complexation were calculated. The $\Delta q(\text{H})$ values were increased by 0.0524–0.1007 au upon complexation.

2.4. Energy Decomposition Analysis. The interactions of MeOH–daidzein, MeOH–genistein, and MeOH–glycitein are very similar. It is necessary to make a detailed inspection to understand the nature of the chemical bonds. Then, the total interaction energies of the most stable conformers of MeOH–daidzein as well as MeOH–genistein and MeOH–glycitein were further studied by the generalized Kohn–Sham energy decomposition analysis (GKS-EDA) (Figure 8). The GKS-EDA reveals that there are five components with negative values, namely, ΔE_{ex} , ΔE_{es} , ΔE_{pol} , ΔE_{dc} and ΔE_{corr} . This means that they are attractive terms, which stabilize the system. Among the attractive terms, the ΔE_{ex} interactions are very important for the hydrogen bonds with large negative values (-93.9 to -85.4 kJ mol $^{-1}$). ΔE_{ex} indicates that charge transfer plays an important role. Moreover, the charge transfer will also affect the electrostatic parameters at the binding site. Thus, the ΔE_{es} interactions (-58.6 to -57.6 kJ mol $^{-1}$) also have a large contribution to the total interaction energies. The largest ΔE_{pol}

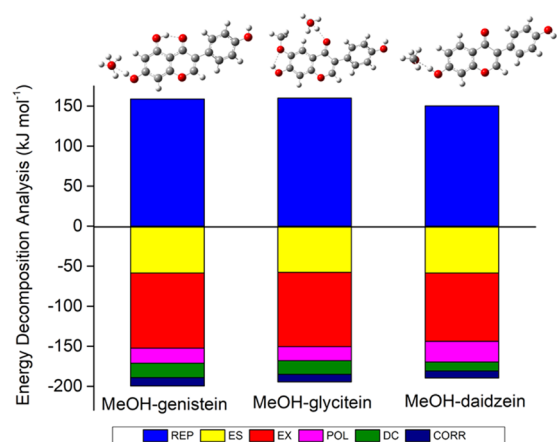


Figure 8. Six components of the total interaction energies in the generalized Kohn–Sham energy decomposition analysis (GKS-EDA) at the B3LYP-D3/cc-pVTZ level.

in MeOH–daidzein suggests a great change in ion pair formation to increase the hydrogen bond interaction. Moreover, the ΔE_{dc} and ΔE_{corr} terms are the smallest proportion of ΔE_{int} . The larger $(\Delta E_{dc} + \Delta E_{corr})/\Delta E_{int}$ term means a larger orbital overlap between the two fragments in the complex. The $(\Delta E_{dc} + \Delta E_{corr})/\Delta E_{int}$ term of MeOH–genistein is 0.70, which is larger than those of MeOH–glycitein (0.66) and MeOH–daidzein (0.51). The ΔE_{rep} energies are positive values; they suggest that the orbital overlap plays an important role in destabilizing the system. The ΔE_{rep} energy of MeOH–glycitein is slightly larger ($159.8 \text{ kJ mol}^{-1}$) than those of MeOH–genistein ($158.8 \text{ kJ mol}^{-1}$) and MeOH–daidzein ($150.3 \text{ kJ mol}^{-1}$).

2.5. Gibbs Free Energy. Thermodynamic properties can provide profound insights into molecular interactions to interpret solute–solvent interactions. On the other hand, the macroscopic state of the system is also displayed by the average fundamental thermodynamic properties of individual microscopic states, such as Gibbs free energy of formation.³⁰ Moreover, thermodynamic properties, such as Gibbs free energy of formation, are often utilized to reveal the spontaneity of a molecular interaction process. If the total Gibbs free energy of formation of the system decreases during the reaction, it is a spontaneous process. Thus, the change in Gibbs free energy of formation is an important factor to measure the spontaneity. Since daidzein, genistein, and glycitein are the most common soybean isoflavones, it is also interesting to compare their properties during extraction. The electronic energies of the most stable conformers of MeOH–daidzein as well as MeOH–genistein/glycitein were calculated on the top of the optimized structures, using single-point calculations at the B3LYP-D3/cc-pVTZ level of theory. Usually, one can decrease the temperature to increase the efficiency of extraction.³¹ In this study, the Gibbs free energies of hydrogen bond formation in solution were simulated at various temperatures (278–338 K). The Gibbs free energies of formation of MeOH–daidzein, MeOH–genistein, and MeOH–glycitein are plotted at various temperatures (Figure 9). The results show that an increase in temperature will cause a rise in the Gibbs free energy. Thus, this leads these complexes to be thermodynamically unstable at high temperatures. According to the simulations, the extraction temperature for genistein should be below 321 K; then it should be

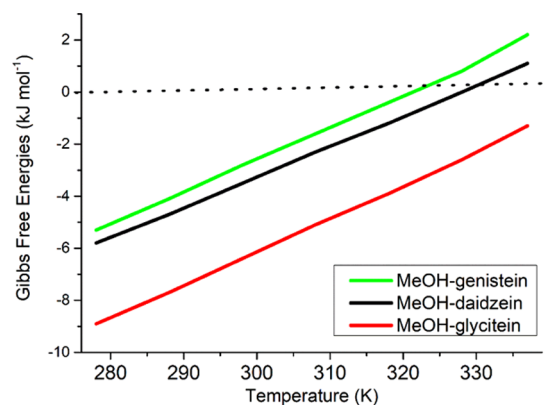


Figure 9. Gibbs free energy of formation of MeOH–genistein, MeOH–glycitein, and MeOH–daidzein as a function of temperature during extraction.

below 328 K for daidzein. The MeOH–glycitein complex is the most stable one, and the extraction temperature for glycitein can be under 348 K.

3. CONCLUDING REMARKS

In this study, the interactions between daidzein and MeOH as an extraction solvent were investigated. The daidzein molecule is characterized by four docking sites, which makes it suitable for hydrogen bond formation. The four docking sites of the daidzein molecule are oxygen atoms, which act as hydrogen bond acceptors. The daidzein molecule also acts as a hydrogen bond donor by the two hydrogen atoms found in the hydroxyl groups. According to the calculations, daidzein prefers to act as a hydrogen bond donor than a hydrogen bond acceptor. More MeOH molecules interacting with daidzein could give extra stability in binding energy. The strengths of the attractive solute–solvent and solute–solute interactions were studied to elucidate the extraction process by considering electrostatic, repulsion, polarization, exchange, DFT correlation, and Grimme dispersion energies. The solute–solute π – π stacking interactions are much stronger than the solute–solute hydrogen-bonding interactions. This study also sought to assess the phase separation from a microscopic viewpoint, using Gibbs free energies as compared to other isoflavones like glycitein and genistein. According to calculations, the extraction temperatures by MeOH should be below about 321, 328, and 348 K for genistein, daidzein, and glycitein, respectively. In the crystal phase, the solute–solute interactions were discussed.

4. COMPUTATIONAL DETAILS

The Gaussian 09 program (revision E.01) was used for all geometry optimizations and vibrational frequency calculations.³² DFT has been widely used in predicting the chemical and physical properties of biomolecules, such as coumarin, glycitein, genistein, etc.^{7,8,33} Based on the results of previous studies, the DFT calculations employing the Becke three-parameter and Lee–Yang–Parr hybrid functional with the D3 version of Grimme’s dispersion (B3LYP-D3) showed a fine performance on small bimolecular and trimolecular clusters, and its predictions agree best with experiments compared to other density functionals.^{34–36} For all of the DFT calculations, the cc-pVTZ basis set was used as it is a good compromise between accuracy and efficiency and does not yield significant

errors in the thermal contribution to the free energy.^{7,8} The additional options “opt = verytight” and “integral = ultrafine” were included in all of the optimization calculations. These two options have been shown to give good frequencies and thermochemical corrections to the electronic energies for the hydrogen-bonded complexes.³⁷ For each stationary point, frequency calculations confirmed that no imaginary frequencies existed. The binding energies (BEs) were calculated as the energy difference between the complex and the sum of the monomers. Zero-point vibrational energies (ZPVEs) were employed for the correction of BEs.

The strength and nature of noncovalent interactions, such as hydrogen bond and π - π , would be different. The physical nature of the noncovalent interaction needs to be studied in depth to obtain a reasonable description of the components of the total noncovalent interaction energy using the generalized Kohn–Sham energy decomposition analysis (GKS-EDA) method as implemented in the GAMESS-US (version R1) program.^{38,39} Then, the total interaction energy ΔE_{int} can be decomposed into a number of physically meaningful components: electrostatic energy (ΔE_{es}), repulsion energy (ΔE_{rep}), polarization energy (ΔE_{pol}), exchange energy (ΔE_{ex}), DFT correlation (ΔE_{corr}), and Grimme dispersion energy (ΔE_{dc}). The AIM2000 package at the B3LYP-D3/cc-pVTZ level was engaged for topological analysis, which was performed using atoms in molecules (AIM) theory to investigate the nature of hydrogen-bonded complexes.⁴⁰ The topological properties (e.g., charge density $\rho(r)$ and the Laplacian of charge density $\nabla^2\rho(r)$) at bond critical points (BCPs) were applied to evaluate the individual hydrogen bond strength in the hydrogen-bonded complexes.

AUTHOR INFORMATION

Corresponding Author

Xia Sheng – College of Sciences, Henan Agricultural University, 450002 Zhengzhou, China; orcid.org/0000-0002-4831-5138; Email: shengxia@henau.edu.cn

Authors

Hailiang Zhao – School of Environmental Engineering, Henan University of Technology, 450001 Zhengzhou, China; College of Sciences, Henan Agricultural University, 450002 Zhengzhou, China; orcid.org/0000-0001-8855-4611

Zhenjun Wu – School of Environmental Engineering, Henan University of Technology, 450001 Zhengzhou, China

Yaming Sun – School of Environmental Engineering, Henan University of Technology, 450001 Zhengzhou, China

Xue Song – School of Environmental Engineering, Henan University of Technology, 450001 Zhengzhou, China

Fan Shi – School of Environmental Engineering, Henan University of Technology, 450001 Zhengzhou, China

Yingming Zhang – School of Environmental Engineering, Henan University of Technology, 450001 Zhengzhou, China

Complete contact information is available at:

<https://pubs.acs.org/10.1021/acsomega.1c02348>

Notes

The authors declare no competing financial interest.

ACKNOWLEDGMENTS

Financial support for this work was provided by the Key Science and Technology Program of Henan Province under Grant number 202102210056, the Cultivation Programme for

Young Backbone Teachers in Henan University of Technology, Henan University of Technology under Grant number 2017BS046, the Student's Platform for Innovation and Entrepreneurship Training Program of Henan Province under Grant numbers 201910463050 and 202010463023, and the Fundamental Research Funds for the Henan Provincial Colleges and Universities in Henan University of Technology under Grant number 2017QNJH27, the Natural Science Innovation Fund of Henan University of Technology under Grant number 2020ZKJC30. The authors thank the High Performance Computing Centre of Shandong University for providing the Gaussian 09, revision E.01 software package and high-performance computation. The authors also thank Prof. Peifeng Su from Xiamen University for providing the generalized Kohn–Sham energy decomposition analysis (GKS-EDA) software package.

REFERENCES

- (1) Abraham, M. H.; Acree, W. E., Jr.; Earp, C. E.; Vladimirova, A.; Whaley, W. L. Studies on the Hydrogen Bond Acidity, and Other Descriptors and Properties for Hydroxyflavones and Hydroxyisoflavones. *J. Mol. Liq.* **2015**, *208*, 363–372.
- (2) Dong, X.; Cao, Y.; Lin, H.; Yao, Y.; Guo, Y.; Wang, T.; Wu, S.; Wu, Z. Solubilities of Formononetin and Daidzein in Organic Solvents: Effect of Molecular Structure and Interaction on Solvation Process. *J. Mol. Liq.* **2017**, *231*, 542–554.
- (3) Touden, Y.; Ishiwata, H.; Takeda, K.; Ishimi, Y. Assessment of Safety and Efficacy of Perinatal or Peripubertal Exposure to Daidzein on Bone Development in Rats. *Toxicol. Rep.* **2015**, *2*, 429–436.
- (4) Singh, H.; Singh, S.; Srivastava, A.; Tandon, P.; Bharti, P.; Kumar, S.; Maurya, R. Conformational Analysis and Vibrational Study of Daidzein by Using FT-IR and FT-Raman Spectroscopies and DFT Calculations. *Spectrochim. Acta, Part A* **2014**, *120*, 405–415.
- (5) Cheong, S. H.; Furuhashi, K.; Ito, K.; Nagaoka, M.; Yonezawa, T.; Miura, Y.; Yagasaki, K. Daidzein Promotes Glucose Uptake through Glucose Transporter 4 Translocation to Plasma Membrane in L6 Myocytes and Improves Glucose Homeostasis in Type 2 Diabetic Model Mice. *J. Nutr. Biochem.* **2014**, *25*, 136–143.
- (6) Dong, K.; Cao, Y.; Yang, Q.; Zhang, S.; Xing, H.; Ren, Q. Role of Hydrogen Bonds in Ionic-Liquid-Mediated Extraction of Natural Bioactive Homologues. *Ind. Eng. Chem. Res.* **2012**, *51*, 5299–5308.
- (7) Zhao, H.; Song, X.; Zhang, Y.; Sheng, X.; Gu, K. Molecular Understanding of Solvents and Glycitein Interaction during Extraction. *ACS Omega* **2019**, *4*, 17823–17829.
- (8) Zhao, H.; Song, X.; Zhang, Y.; Sheng, X. Molecular Interaction between MeOH and Genistein during Soy Extraction. *RSC Adv.* **2019**, *9*, 39170–39179.
- (9) Wu, Q.; Wang, M.; Simon, J. E. Determination of Isoflavones in Red Clover and Related Species by High-performance Liquid Chromatography Combined with Ultraviolet and Mass Spectrometric Detection. *J. Chromatogr. A* **2003**, *1016*, 195–209.
- (10) Bustamante-Rangel, M.; Delgado-Zamarreño, M. M.; Carabias-Martínez, R.; Domínguez-Álvarez, J. Analysis of Isoflavones in Soy Drink by Capillary Zone Electrophoresis Coupled with Electrospray Ionization Mass Spectrometry. *Anal. Chim. Acta* **2012**, *709*, 113–119.
- (11) Zafrá-Gómez, A.; Garballo, A.; García-Ayuso, L. E.; Morales, J. C. Improved Sample Treatment and Chromatographic Method for the Determination of Isoflavones in Supplemented Foods. *Food Chem.* **2010**, *123*, 872–877.
- (12) Zuo, Y. B.; Zeng, A. W.; Yuan, X. G.; Yu, K. T. Extraction of Soybean Isoflavones from Soybean Meal with Aqueous Methanol Modified Supercritical Carbon Dioxide. *J. Food Eng.* **2008**, *89*, 384–389.
- (13) Luthria, D. L.; Biswas, R.; Natarajan, S. Comparison of Extraction Solvents and Techniques Used for the Assay of Isoflavones from Soybean. *Food Chem.* **2007**, *105*, 325–333.

- (14) Song, T. T.; Hendrich, S.; Murphy, P. A. Estrogenic Activity of Glycitein, a Soy Isoflavone. *J. Agric. Food Chem.* **1999**, *47*, 1607–1610.
- (15) Jia, L.; Xu, S.; Liu, S.; Du, S.; Wu, S.; Gong, J. Polymorphs of Daidzein and Intermolecular Interaction Effect on Solution Crystallization. *CrystEngComm* **2017**, *19*, 7146–7153.
- (16) Du, W.; Yin, Q. X.; Hao, H. X.; Bao, Y.; Zhang, X.; Huang, J. T.; Li, X.; Xie, C.; Gong, J. B. Solution-Mediated Polymorphic Transformation of Prasugrel Hydrochloride from Form II to Form I. *Ind. Eng. Chem. Res.* **2014**, *53*, 5652–5659.
- (17) Gu, C. H.; Young, V., Jr.; Grant, D. J. Polymorph Screening: Influence of Solvents on the Rate of Solvent-mediated Polymorphic Transformation. *J. Pharm. Sci.* **2001**, *90*, 1878–90.
- (18) Du, W.; Yin, Q. X.; Gong, J. B.; Bao, Y.; Zhang, X.; Sun, X. W.; Ding, S. P.; Xie, C.; Zhang, M. J.; Hao, H. X. Effects of Solvent on Polymorph Formation and Nucleation of Prasugrel Hydrochloride. *Cryst. Growth Des.* **2014**, *14*, 4519–4525.
- (19) Du, L.; Tang, S.; Hansen, A. S.; Frandsen, B. N.; Maroun, Z.; Kjaergaard, H. G. Subtle Differences in the Hydrogen Bonding of Alcohol to Divalent Oxygen and Sulfur. *Chem. Phys. Lett.* **2017**, *667*, 146–153.
- (20) Du, L.; Mackeprang, K.; Kjaergaard, H. G. Fundamental and Overtone Vibrational Spectroscopy, Enthalpy of Hydrogen Bond Formation and Equilibrium Constant Determination of the Methanol-Dimethylamine Complex. *Phys. Chem. Chem. Phys.* **2013**, *15*, 10194–10206.
- (21) Zhao, H.; Tang, S.; Du, L. Hydrogen Bond Docking Site Competition in Methyl Esters. *Spectrochim. Acta A* **2017**, *181*, 122–130.
- (22) Tsuzuki, S.; Uchamaru, T.; Matsumura, K.; Mikami, M.; Tanabe, K. Effects of Basis Set and Electron Correlation on the Calculated Interaction Energies of Hydrogen Bonding Complexes: MP2/cc-pV5Z Calculations of H₂O–MeOH, H₂O–Me₂O, H₂O–H₂CO, MeOH–MeOH, and HCOOH–HCOOH Complexes. *J. Chem. Phys.* **1999**, *110*, 11906–11910.
- (23) Sinnokrot, M. O.; Sherrill, C. D. High-Accuracy Quantum Mechanical Studies of π – π Interactions in Benzene Dimers. *J. Phys. Chem. A* **2006**, *110*, 10656–10668.
- (24) Feng, C.; Lin, C.; Zhang, X.; Zhang, R. π – π Interaction in Benzene Dimer Studied Using Density Functional Theory Augmented with an Empirical Dispersion Term. *J. Theor. Comput. Chem.* **2010**, *09*, 109–123.
- (25) Koch, U.; Popelier, P. Characterization of CHO Hydrogen Bonds on the Basis of the Charge Density. *J. Phys. Chem. A* **1995**, *99*, 9747–9754.
- (26) Grabowski, S. J. Hydrogen Bonding Strength-Measures Based on Geometric and Topological Parameters. *J. Phys. Org. Chem.* **2004**, *17*, 18–31.
- (27) Blanco, S.; Pinacho, P.; López, J. C. Hydrogen-Bond Cooperativity in Formamide₂–Water: A Model for Water-Mediated Interactions. *Angew. Chem., Int. Ed.* **2016**, *55*, 9477–9481.
- (28) Mahadevi, A. S.; Sastry, G. N. Cooperativity in Noncovalent Interactions. *Chem. Rev.* **2016**, *116*, 2775–2825.
- (29) Bushmarinov, I. S.; Lyssenko, K. A.; Antipin, M. Y. Atomic Energy in the ‘Atoms in Molecules’ Theory and its Use for Solving Chemical Problems. *Russ. Chem. Rev.* **2009**, *78*, 283–302.
- (30) Ankita; Nain, A. K. Solute-solute and Solute-solvent Interactions of Drug Sodium Salicylate in Aqueous-glucose/sucrose Solutions at Temperatures from 293.15 to 318.15 K: A Physicochemical Study. *J. Mol. Liq.* **2020**, *298*, No. 112006.
- (31) Kumhom, T.; Elkamel, A.; Douglas, P. L.; Douglas, S.; Pongamphai, S.; Teppaitoon, W. Prediction of Isoflavone Extraction from Soybean Meal Using Supercritical Carbon Dioxide with Cosolvents. *Chem. Eng. J.* **2011**, *172*, 1023–1032.
- (32) Frisch, M. J.; Trucks, G. W.; Schlegel, H. B.; Scuseria, G. E.; Robb, M. A.; Cheeseman, J. R.; Scalmani, G.; Barone, V.; Mennucci, B.; Petersson, G. A.; Nakatsuji, H.; Caricato, M.; Li, X.; Hratchian, H. P.; Izmaylov, A. F.; Bloino, J.; Zheng, G.; Sonnenberg, J. L.; Hada, M.; Ehara, M.; Toyota, K.; Fukuda, R.; Hasegawa, J.; Ishida, M.; Nakajima, T.; Honda, Y.; Kitao, O.; Nakai, H.; Vreven, T.; Montgomery, J. A., Jr.; Peralta, J. E.; Ogliaro, F.; Bearpark, M. J.; Heyd, J.; Brothers, E. N.; Kudin, K. N.; Staroverov, V. N.; Kobayashi, R.; Normand, J.; Raghavachari, K.; Rendell, A. P.; Burant, J. C.; Iyengar, S. S.; Tomasi, J.; Cossi, M.; Rega, N.; Millam, N. J.; Klene, M.; Knox, J. E.; Cross, J. B.; Bakken, V.; Adamo, C.; Jaramillo, J.; Gomperts, R.; Stratmann, R. E.; Yazyev, O.; Austin, A. J.; Cammi, R.; Pomelli, C.; Ochterski, J. W.; Martin, R. L.; Morokuma, K.; Zakrzewski, V. G.; Voth, G. A.; Salvador, P.; Dannenberg, J. J.; Dapprich, S.; Daniels, A. D.; Farkas, Ö.; Foresman, J. B.; Ortiz, J. V.; Cioslowski, J.; Fox, D. J. *Gaussian 09*, revision E.01; Gaussian, Inc.: Wallingford, CT, 2013.
- (33) Milenković, D. A.; Dimić, D. S.; Avdović, E. H.; Amić, A. D.; Dimitrić Marković, J. M.; Marković, Z. S. Advanced Oxidation Process of Coumarins by Hydroxyl Radical: Towards the New Mechanism Leading to Less Toxic Products. *Chem. Eng. J.* **2020**, *395*, No. 124971.
- (34) Tang, S.; Du, L. Effects of Methylation in Acceptors on the Hydrogen Bond Complexes between 2,2,2-Trifluoroethanol and Cyclic Ethers. *Spectrochim. Acta A* **2019**, *217*, 237–246.
- (35) Tang, S.; Tsona, N. T.; Du, L. Ring-Size Effects on the Stability and Spectral Shifts of Hydrogen Bonded Cyclic Ethers Complexes. *Sci. Rep.* **2018**, *8*, No. 1553.
- (36) Jiang, X.; Tsona, N. T.; Tang, S.; Du, L. Hydrogen Bond Docking Preference in Furans: OH $\cdots\pi$ vs. OH \cdots O. *Spectrochim. Acta A* **2018**, *191*, 155–164.
- (37) Sheng, X.; Song, X.; Ngwenya, C. A.; Wang, Y.; Zhao, H. Atmospheric Initial Nucleation Containing Carboxylic Acids. *J. Phys. Chem. A* **2019**, *123*, 3876–3886.
- (38) Schmidt, M. W.; Baldrige, K. K.; Boatz, J. A.; Elbert, S. T.; Gordon, M. S.; Jensen, J. H.; Koseki, S.; Matsunaga, N.; Nguyen, K. A.; Su, S.; Windus, T. L.; Dupuis, M.; Montgomery, J. A. General Atomic and Molecular Electronic Structure System. *J. Comput. Chem.* **1993**, *14*, 1347–1363.
- (39) Su, P.; Li, H. Energy Decomposition Analysis of Covalent Bonds and Intermolecular Interactions. *J. Chem. Phys.* **2009**, *131*, No. 014102.
- (40) Lane, J. R.; Contreras-Garcia, J.; Piquemal, J.-P.; Miller, B. J.; Kjaergaard, H. G. Are Bond Critical Points Really Critical for Hydrogen Bonding? *J. Chem. Theory Comput.* **2013**, *9*, 3263–3266.